Chinese Journal of Aeronautics 24 (2011) 32-45

Contents lists available at ScienceDirect

Chinese Journal of Aeronautics

journal homepage: www.elsevier.com/locate/cja

Adaptive Integral-type Sliding Mode Control for Spacecraft Attitude Maneuvering Under Actuator Stuck Failures

HU Qinglei[a,b,*], ZHANG Youmin[b], HUO Xing[a], XIAO Bing[a]

[a]*Department of Control Science and Engineering, Harbin Institute of Technology, Harbin 150001, China*

[b]*Department of Mechanical and Industrial Engineering, Concordia University, Montreal H3G 2W1, Canada*

Received 19 August 2010; revised 25 October 2010; accepted 4 November 2010

Abstract

A fault tolerant control (FTC) design technique against actuator stuck faults is investigated using integral-type sliding mode control (ISMC) with application to spacecraft attitude maneuvering control system. The principle of the proposed FTC scheme is to design an integral-type sliding mode attitude controller using on-line parameter adaptive updating law to compensate for the effects of stuck actuators. This adaptive law also provides both the estimates of the system parameters and external disturbances such that a prior knowledge of the spacecraft inertia or boundedness of disturbances is not required. Moreover, by including the integral feedback term, the designed controller can not only tolerate actuator stuck faults, but also compensate the disturbances with constant components. For the synthesis of controller, the fault time, patterns and values are unknown in advance, as motivated from a practical spacecraft control application. Complete stability and performance analysis are presented and illustrative simulation results of application to a spacecraft show that high precise attitude control with zero steady-error is successfully achieved using various scenarios of stuck failures in actuators.

Keywords: integral sliding mode control; attitude maneuvering; stuck failure; adaptive control; spacecraft

1. Introduction

Accurate and reliable control of spacecraft is a major challenge for achieving orbital missions. For this kind of space vehicles, dynamical models are nonlinear and include several disturbance torques, such as those arising from gravity gradient, solar radiation pressure, etc. Moreover, in a practical situation, parameters of spacecraft are not precisely known. In addition, anticipated missions of spacecraft during operation will also require certain levels of safety and fault tolerance to system failures, especially, the case of actuator failures. All these in a realistic environment create considerable difficulty in the design of attitude control system for meeting high precision pointing requirements, especially when all these issues are treated simultaneously.

In the face of various environmental disturbances and increasingly complex and highly uncertain nature of spacecraft dynamical systems in the design of control systems for spacecraft, many studies related to attitude control of spacecraft have been done, and robust linear and nonlinear control systems have been designed. Control laws based on linearization and nonlinear inversion have been presented in Ref.[1]. Optimal and nonlinear control systems for the control of spacecraft have been developed in Refs.[2]-[3]. Based on Lyapunov stability and dissipativity theory,

*Corresponding author. Tel.: +86-451-86402726.
E-mail address: huqinglei@hit.edu.cn

Foundation items: National Natural Science Foundation of China (61004072); Fundamental Research Funds for the Central Universities (HIT.NSRIF.2009003); Research Fund for the Doctoral Program of Higher Education of China (20070213061, 20102302110031); Scientific Research Foundation for the Returned Overseas Chinese Scholars of Harbin (2010RFLXG001)

doi: 10.1016/S1000-9361(11)60005-8

dynamic attitude control laws for spacecraft have been designed in Refs.[4]-[5]. Sliding mode control (SMC) to certain types of disturbances and uncertainties also makes it attractive for spacecraft control problems and many relative works have been attempted in Refs.[6]-[8] and the references therein. However, these design methods require the information on the bounds of the uncertainties/disturbances for the computation of the controller gains. Unlike these methods, nonlinear adaptive control methods do not require these bounds, instead, by including an adaptation mechanism for tuning the time-varying controller gains. A variety of adaptive spacecraft controllers have been developed[9-10]. Researches have also been focused on the combination of SMC and adaptive control to develop simple and adaptive robust spacecraft controllers that work for a wide range of practical systems[11-14]. However, the methods mentioned above did not explicitly investigate the effects of constant disturbance torques on the attitude regulation. Elimination of offsets arising out of such disturbances using the linear and/or nonlinear controllers without integral term requires very high proportional gains that are undesirable. A nonlinear proportional-derivative (PD) by ingeniously incorporating a modified integral variable was developed by Subbarao[15] through a special Lyapunov function construction involving quadratic cross state weighting such that globally asymptotical attitude convergence to zero was achieved. In Ref.[16], a backstepping-based sliding mode control scheme with integral term was discussed for the flexible spacecraft attitude system design with external disturbances including constant component. However, most (if not all) of the previous research work can hardly be extended to the spacecraft control system when the actuator faults are taken into account explicitly, especially with the kind of stuck failures as additional constant disturbances imposed on the system.

For accommodating actuator faults automatically to achieve high reliability and availability for spacecraft control systems, a control law with fault tolerant capability, called fault tolerant control (FTC), could be a desirable one. FTC is an area of research that emerges to increase availability by specifically designing control algorithms capable of maintaining stability and performance despite the occurrence of faults, and has received considerable attention from the control research community and aeronautical engineering in the past couple of decades[17-18]. The available design techniques include the linear quadratic control method[19], adaptive control[20-21], eigenstructure assignment[22] and SMC[23-24], to name a few. As for the application of FTC to spacecraft attitude control system design, in Ref.[25], Bošković, et al. used multiple-model method to detect and isolate actuator faults for spacecraft attitude control system. Based on dynamically driven recurrent neural network architecture, a fault detection and isolation (FDI) strategy was proposed for satellite's attitude control system when the thruster failures occurred[26]. In Ref.[27], a robust FDI method based on neural state-space models was applied to a satellite attitude control subsystem, and the robustness, sensitivity and stability properties of this method were investigated. Chen and Saif[28] presented a fault diagnosis approach in satellite system for identifying thruster faults by using an iterative learning observer. In Ref.[29], the authors used the dynamic inversion and time-delay theory to design a passive fault-tolerant controller for a rigid satellite with four reaction wheels to achieve the attitude tracking control. To take into account the redundant thrusters, an indirect adaptive FTC for attitude tracking of rigid spacecraft is proposed in the presence of unknown uncertainties, disturbances and actuator failures, in which a bounded parameter of the lumped perturbations is introduced to be updated on-line[30]. In Ref.[31], an adaptive sliding mode-based FTC with L_2-gain performance was developed for the flexible spacecraft attitude control system wherein the persistently bounded disturbances and unknown inertia parameter uncertainties were explicitly taken into account.

Although FTC for spacecraft system has been extensively studied, to the best knowledge of the authors, so far few articles have been devoted to an especially serious fault scenario, stuck actuators. Once stuck, the actuators can no longer respond to control signals, and it is difficult to deal with stuck actuator failures because the remaining actuators must compensate for the effects of the failed actuators in the overall system. Ref.[32] suggested a control reconfiguration method using an iterative learning observer to accommodate stuck actuators. A reconfigurable control law with adjustable parameters is designed using the observed system state information. In Ref.[33], actuator stuck faults including the outage of partial actuators are considered. Through designing an output feedback controller with an additional weighting matrix, the closed-loop system is stabilized for both fault-free and faulty cases, and a steady-state-based fault detection approach is proposed such that arbitrary small stuck actuator faults can be detected effectively. Stuck actuator faults have also been treated as constant disturbances in Ref.[34] where a proportional-integral (PI) controller is used to reject their effects. An H_∞ controller is designed and an iterative linear matrix inequality (LMI)-based algorithm is used in Ref.[35]. The design is such that the nominal performance is optimized and the closed-loop system performance under different fault modes is acceptable.

In this article, an attempt is made to provide a FTC strategy for the spacecraft with redundant actuators, such as four or more thrusters which are commonly used for attitude control, to address the aforementioned issues. The proposed control strategy is based on an adaptive integral sliding mode control theory and it is applied to the spacecraft suffering from unknown stuck failures of thrusters, external disturbances, and unknown inertia matrix of spacecraft. A key feature of the proposed strategy is that the design of the FTC is done independently of the information of faults and the upper bounds of external disturbances are not required either. A stability condition is also provided such that the proposed fault tolerant controller guarantees that the closed-loop is globally asymptotically stable by the Lyapunov-like stability analysis. Finally, applications are carried out on an orbiting spacecraft with flexible appendages.

2. Mathematical Model of a Spacecraft

2.1. Kinematic equation

In this work, the unit quaternion is adopted to describe the attitude of a rigid spacecraft for global representation without singularities. The attitude kinematics in term of unit quaternion is given as[36]

$$\begin{bmatrix} \dot{q}_0 \\ \dot{\boldsymbol{q}} \end{bmatrix} = \frac{1}{2}\boldsymbol{Q}(q_0,\boldsymbol{q})\boldsymbol{\omega} \tag{1a}$$

$$\boldsymbol{Q}(q_0,\boldsymbol{q}) = [-\boldsymbol{q} \quad q_0\boldsymbol{I} + \boldsymbol{q}^{\times}]^{\mathrm{T}} \tag{1b}$$

where q_0 and $\boldsymbol{q}$ are the scalar and vector components of the unit quaternion respectively, with $\boldsymbol{q}=[q_1 \ q_2 \ q_3]^{\mathrm{T}}\in\mathbf{R}^3$, $\boldsymbol{\omega}\in\mathbf{R}^3$ is the angular velocity of a body-fixed reference frame of a spacecraft with respect to an inertial reference frame expressed in the body-fixed reference frame, $\boldsymbol{I}$ the identity matrix with proper dimensions, and $\boldsymbol{q}^{\times}$ a skew-symmetric matrix which satisfies

$$\boldsymbol{q}^{\times} = \begin{bmatrix} 0 & -q_3 & q_2 \\ q_3 & 0 & -q_1 \\ -q_2 & q_1 & 0 \end{bmatrix} \tag{2}$$

Note that the unit quaternion is subject to the constraint $\boldsymbol{q}^{\mathrm{T}}\boldsymbol{q}+q_0=1$. It can be easily verified from the preceding definition that

$$\boldsymbol{Q}^{\mathrm{T}}\boldsymbol{Q}=\boldsymbol{I}_3, \quad \boldsymbol{Q}^{\mathrm{T}}\begin{bmatrix} q_0 \\ \boldsymbol{q} \end{bmatrix}=\boldsymbol{0}$$

These properties will be used in the following development. Note that since the unit quaternion parameter set $[q_0 \quad \boldsymbol{q}^{\mathrm{T}}]^{\mathrm{T}}$ given in Eq.(1) is redundant, a given physical attitude for a rigid body will have two mathematical representations, where one of these includes a rotation of $\pm 2\pi$ about an axis relative to the other. Therefore, if $[1 \quad \boldsymbol{0}^{\mathrm{T}}]^{\mathrm{T}}$ represents the desired equilibrium point, then $[-1 \quad \boldsymbol{0}^{\mathrm{T}}]^{\mathrm{T}}$ represents the same attitude after a rotation of $\pm 2\pi$ about an arbitrary axis. In the following, only $[1 \quad \boldsymbol{0}^{\mathrm{T}}]^{\mathrm{T}}$ is considered as the desired attitude equilibrium point for the controller design synthesis.

2.2. Dynamic equation with actuator stuck failure

The dynamic model of a spacecraft is governed by the following differential equation[36]:

$$\boldsymbol{J}\dot{\boldsymbol{\omega}} + \boldsymbol{\omega}\times(\boldsymbol{J}\boldsymbol{\omega}) = \boldsymbol{D}\boldsymbol{F}(t) + \boldsymbol{T}_{\mathrm{d}} \tag{3}$$

where $\boldsymbol{J}=\boldsymbol{J}^{\mathrm{T}}\in\mathbf{R}^{3\times3}$ denotes the inertia matrix of the rigid spacecraft expressed in the body-fixed reference frame, $\boldsymbol{F}(t)\in\mathbf{R}^{l}$ the control propulsion force vector produced by l thrusters, and $\boldsymbol{D}\in\mathbf{R}^{3\times l}$ the thruster distribution matrix representing the influence of each thruster on the angular acceleration of the spacecraft. Note that for a given spacecraft, the matrix $\boldsymbol{D}$ is available and can be made full-row rank by properly placing the thrusters at certain locations and directions on the spacecraft. In addition, $\boldsymbol{T}_{\mathrm{d}}=[T_{\mathrm{d}1} \quad T_{\mathrm{d}2} \quad T_{\mathrm{d}3}]^{\mathrm{T}}\in\mathbf{R}^3$ represents the external disturbance torques due to gravitation, solar radiation, magnetic forces, etc., and it is reasonable to assume that the disturbances are bounded.

To formulate the FTC problem of this work, the following type fault model is adopted. Here it is assumed that the remaining active actuators are fault-free and able to produce a combined force sufficient enough to allow the spacecraft to perform given maneuvers at the same time. When stuck failures occur, the input signals of the system are given by

$$\boldsymbol{F}(t) = \boldsymbol{E}\boldsymbol{u} + (\boldsymbol{I}-\boldsymbol{E})\boldsymbol{F}_{\mathrm{f}} \tag{4}$$

where $\boldsymbol{F}_{\mathrm{f}}=[F_{\mathrm{f},1} \ \cdots \ F_{\mathrm{f},i} \ \cdots \ F_{\mathrm{f},l}]^{\mathrm{T}}$ with $\underline{F}_{\mathrm{f},i}\le F_{\mathrm{f},i}\le \overline{F}_{\mathrm{f},i}$ being a zero or nonzero constant which denotes the stuck value of the ith actuator, $\underline{F}_{\mathrm{f},i}$ and $\overline{F}_{\mathrm{f},i}$ are known scalars, and the vector $\boldsymbol{u}$ denotes the designed propulsion force vector. The diagonal matrix $\boldsymbol{E}$ satisfies

$$\boldsymbol{E} = \mathrm{diag}(e_1, e_2, \cdots, e_l) \tag{5}$$

with $e_i=0$ or $e_i=1$ ($i=1,2,\cdots,l$). Obviously, $e_i=0$ for any $1\le i\le l$, the fault model corresponds to the case, when the ith thruster gets faulty, particularly, if the stuck value $\underline{F_{\mathrm{f},i}=0}$, the model denotes an important case: outage. If $e_i=1$, the ith actuator is fault-free.

In view of the stuck failure given by Eq.(4), the system Eq.(3) can be rewritten as

$$\boldsymbol{J}\dot{\boldsymbol{\omega}} + \boldsymbol{\omega}\times(\boldsymbol{J}\boldsymbol{\omega}) = \boldsymbol{D}\boldsymbol{E}\boldsymbol{u} + \boldsymbol{D}(\boldsymbol{I}-\boldsymbol{E})\boldsymbol{F}_{\mathrm{f}} + \boldsymbol{T}_{\mathrm{d}} \tag{6}$$

Note that the effect of stuck actuators can be considered as additional constant disturbances imposed on the system, which may drive the attitude away from the desired position. The closed-loop system stability may also be affected due to the loss of some control channels. In order to return to its original position, the remaining actuators must be adjusted accordingly, to counteract the effect of the stuck actuators and the change in the dynamics as the result of such a failure.

In order to develop the controller, the transformation technique addressed in Ref.[37] is used here for the system Eq.(6), and then the following dynamic equations are given as follows:

$$\boldsymbol{J}^{*}(\boldsymbol{q},q_0)\ddot{\boldsymbol{q}} + \boldsymbol{C}^{*}(\dot{\boldsymbol{q}},\boldsymbol{q},q_0)\dot{\boldsymbol{q}} = \frac{1}{2}\boldsymbol{P}\boldsymbol{D}\boldsymbol{E}\boldsymbol{u} + \frac{1}{2}\boldsymbol{P}[\boldsymbol{T}_{\mathrm{d}} + \boldsymbol{D}(\boldsymbol{I}-\boldsymbol{E})\boldsymbol{F}_{\mathrm{f}}] \tag{7a}$$

$$\dot{\boldsymbol{q}} = \frac{1}{2}\boldsymbol{\Xi}\boldsymbol{\omega} \tag{7b}$$

$$\boldsymbol{J}^*(\boldsymbol{q}, q_0) \triangleq \boldsymbol{P}^{\mathrm{T}}\boldsymbol{J}\boldsymbol{P} \tag{7c}$$

$$\boldsymbol{C}^*(\dot{\boldsymbol{q}}, \boldsymbol{q}, q_0) \triangleq -\boldsymbol{J}^*\dot{\boldsymbol{P}}^{-1}\boldsymbol{P} - 2\boldsymbol{P}^{\mathrm{T}}(\boldsymbol{J}\boldsymbol{P}\dot{\boldsymbol{q}})^{\times}\boldsymbol{P} \tag{7d}$$

where $\boldsymbol{\Xi} \equiv \boldsymbol{q}^{\times} + q_0\boldsymbol{I}$ and $\boldsymbol{P} \equiv \boldsymbol{\Xi}^{-1}$. Note that Eq.(7) are the general nonlinear equations of motion for spacecraft with the possible actuator stuck failures and external disturbances, which will be used in the following controller synthesis.

The model in Eq.(7a) has the following properties:

Property 1 The matrix $\boldsymbol{J}^*$ is symmetric positive definite and the matrix $\dot{\boldsymbol{J}}^*(\boldsymbol{q}, q_0) - 2\boldsymbol{C}^*(\dot{\boldsymbol{q}}, \boldsymbol{q}, q_0)$ is skew-symmetric, that is

$$\boldsymbol{x}^{\mathrm{T}}(\dot{\boldsymbol{J}}^*(\boldsymbol{q}, q_0) - 2\boldsymbol{C}^*(\dot{\boldsymbol{q}}, \boldsymbol{q}, q_0))\boldsymbol{x} = \boldsymbol{0}, \quad \forall \boldsymbol{x} \in \mathbf{R}^3 \tag{8}$$

Property 2 The inertia matrix is bounded, i.e., $\|\boldsymbol{J}\| \le a_0$, where a_0 is unknown constant, and there also exists an unknown scalar $a_1 > 0$ such that the following inequality

$$\|\boldsymbol{C}^*\| \le a_1 \|\dot{\boldsymbol{q}}\| \tag{9}$$

is satisfied, where $\|\bullet\|$ denotes the Euclidean norm.

Property 3 With the disturbances considered, it is reasonable to assume that $\boldsymbol{T}_{\mathrm{d}}(t)$ is bounded and satisfies[36]

$$\|\boldsymbol{T}_{\mathrm{d}}\| \le a_2 + a_3\|\dot{\boldsymbol{q}}\|^2 \tag{10}$$

with $a_2>0$ and $a_3>0$ unknown but constant.

3. Fault Tolerant Attitude Controller Design with Stuck Failures

In this section, we present the design procedure to implement adaptive integral sliding mode-based FTC for spacecraft attitude control system. Adaptive control technique deals with situations in which some of the parameters are unknown or slowly time varying, and the basic idea in this method is to estimate these unknown parameters online and then use the estimated ones in place of the unknown ones in the feedback control law. The overall design can be divided into two main steps. Step 1 involves the construction of a sliding surface, containing integral term to ensure that, once the system is restricted to the sliding surface, the spacecraft can be expected to be in the desired position. Step 2 entails the derivation of parameter adaptation laws and feedback control gains that can drive the spacecraft attitude to the sliding surface and maintain it in the manifold.

3.1. Integral-type sliding surface design

The SMC design starts with building a sliding surface in the system state space. The motion of the system along the sliding mode is expected to meet the control requirements with desired robustness to possible bounded disturbances and parametric uncertainties. In this work, the following sliding surface with integral term is considered:

$$\boldsymbol{S} = \dot{\boldsymbol{q}} + \boldsymbol{K}_{\mathrm{P}}\boldsymbol{q} + \boldsymbol{K}_{\mathrm{I}}\int_0^t \boldsymbol{q}\,\mathrm{d}\tau \tag{11}$$

where $\boldsymbol{K}_{\mathrm{P}}$ and $\boldsymbol{K}_{\mathrm{I}}$ are determined such that the sliding mode on $\boldsymbol{S}=\boldsymbol{0}$ is stable, i.e., the convergence of $\boldsymbol{S}$ to zero in turn guarantees that $\boldsymbol{q}$ and $\dot{\boldsymbol{q}}$ also converge to zero. Note that any positive definite $\boldsymbol{K}_{\mathrm{P}}$ and $\boldsymbol{K}_{\mathrm{I}}$ will satisfy this condition. If $\boldsymbol{K}_{\mathrm{I}}=\boldsymbol{0}$ is selected, this kind of sliding surface becomes the conventional linear sliding surface, $\boldsymbol{S} = \dot{\boldsymbol{q}} + \boldsymbol{K}_{\mathrm{P}}\boldsymbol{q}$, as stated in the literature. Moreover, the additional integral provides one more degree of freedom in design than the conventional linear sliding surface. In addition, the introduced integral term will help to reduce the effect of constant disturbances, which will be discussed in later section.

For convenience of control law design, a new variable is introduced as[38]

$$\dot{\boldsymbol{q}}_{\mathrm{r}} = \dot{\boldsymbol{q}} - \boldsymbol{S} \tag{12}$$

Then from the definition of $\boldsymbol{S}$, we have

$$\dot{\boldsymbol{q}}_{\mathrm{r}} = -\boldsymbol{K}_{\mathrm{P}}\boldsymbol{q} - \boldsymbol{K}_{\mathrm{I}}\int_0^t \boldsymbol{q}\,\mathrm{d}\tau \tag{13}$$

By rearranging Eq.7(a), the following can be obtained

$$\boldsymbol{J}^*\dot{\boldsymbol{S}} + \boldsymbol{C}^*\boldsymbol{S} = \frac{1}{2}\boldsymbol{P}\boldsymbol{D}\boldsymbol{E}\boldsymbol{u} + \frac{1}{2}\boldsymbol{P}[\boldsymbol{T}_{\mathrm{d}} + \boldsymbol{D}(\boldsymbol{I} - \boldsymbol{E})\boldsymbol{F}_{\mathrm{f}}] - (\boldsymbol{J}^*\ddot{\boldsymbol{q}}_{\mathrm{r}} + \boldsymbol{C}^*\dot{\boldsymbol{q}}_{\mathrm{r}}) \tag{14}$$

This nonlinear equation will be used to prove stability of the closed-loop system.

3.2. Adaptive FTC law design

The basic idea is to alter the system dynamics along the sliding surface, such that the trajectory of the system is steered onto the sliding manifold described by $\boldsymbol{S}=\boldsymbol{0}$. As stated in Property 2 and Property 3, the system parameters, disturbances and the stuck failures are assumed to be bounded and, therefore, for the convenience of the controller development, the following variables can be introduced:

$$\left.\begin{aligned} \boldsymbol{Y}_1 &= \left[\|(\ddot{\boldsymbol{q}}_{\mathrm{r}} - \lambda\boldsymbol{S})\| \quad \|\dot{\boldsymbol{q}}_{\mathrm{r}}\|\|\dot{\boldsymbol{q}}\|\right]^{\mathrm{T}} \\ \boldsymbol{\Theta}_1 &= [a_0 \quad a_1]^{\mathrm{T}} \end{aligned}\right\} \tag{15a}$$

$$\left.\begin{aligned} \boldsymbol{Y}_2 &= \frac{\|\boldsymbol{P}\|}{2}[1 + \|\boldsymbol{D}\| \quad \|\dot{\boldsymbol{q}}\|^2]^{\mathrm{T}} \\ \boldsymbol{\Theta}_2 &= [a_2 + \|\boldsymbol{F}_{\mathrm{f}}\| \quad a_3]^{\mathrm{T}} \end{aligned}\right\} \tag{15b}$$

where $\lambda > 0$ is given constant to specify the speed of convergence of the system.

To achieve the sliding motion, the following FTC law is proposed:

$$\boldsymbol{u} = -2\boldsymbol{D}^{\mathrm{T}}\boldsymbol{\Xi}(\boldsymbol{KS} + \hat{\alpha}_1 \|\boldsymbol{Y}_1\| \operatorname{sgn} \boldsymbol{S} + \hat{\alpha}_2 \|\boldsymbol{Y}_2\| \operatorname{sgn} \boldsymbol{S}) \tag{16}$$

with the parameter adaption laws[14,38]

$$\left.\begin{aligned} \dot{\hat{\alpha}}_1 &= -\beta_1^2\hat{\alpha}_1 + \gamma_1 \|\boldsymbol{Y}_1\|\|\boldsymbol{S}\| \\ \dot{\beta}_1 &= -K_{\beta_1}\beta_1 \end{aligned}\right\} \tag{17a}$$

$$\left.\begin{aligned} \dot{\hat{\alpha}}_2 &= -\beta_2^2\hat{\alpha}_2 + \gamma_2 \|\boldsymbol{Y}_2\|\|\boldsymbol{S}\| \\ \dot{\beta}_2 &= -K_{\beta_2}\beta_2 \end{aligned}\right\} \tag{17b}$$

where $\boldsymbol{K}$ is a positive definite matrix chosen by the designer, γ_i and K_{β_i} (i=1, 2) are arbitrary positive constants, $\hat{\alpha}_i$ is the parameter estimation of α_i which satisfies $\alpha_i \geq \|\boldsymbol{\Theta}_i\|$ for i=1, 2. In addition, the sign function satisfies

$$\operatorname{sgn} \upsilon = \begin{cases} 1 & \upsilon > 0 \\ 0 & \upsilon = 0 \\ -1 & \upsilon < 0 \end{cases} \tag{18}$$

We then have the following statement.

Theorem 1 Consider the spacecraft attitude control system in Eq.(7a) with the integral-type sliding surface given in Eq.(11). If the control laws in Eqs.(16)-(17) are implemented with the proper parameters, then the closed-loop system is globally asymptotically stable, and the attitude and velocity respectively converge to zero, i.e., $\lim_{t\to\infty}\boldsymbol{q} \to \boldsymbol{0}$, $\lim_{t\to\infty} q_0 \to 1$ and $\lim_{t\to\infty}\boldsymbol{\omega} \to \boldsymbol{0}$.

Proof Define a Lyapunov function candidate

$$V = \frac{1}{2}\boldsymbol{S}^{\mathrm{T}}\boldsymbol{J}^*\boldsymbol{S} + \sum_{i=1}^{2}\frac{1}{2\delta\gamma_i}\tilde{\alpha}_i^2 + \sum_{i=1}^{2}\frac{K_{\beta_i}^{-1}}{8\delta\gamma_i}\alpha_i^2\beta_i^2 \tag{19}$$

where δ>0 is some unknown constant but less than the minimum eigenvalue of matrix $\boldsymbol{DED}^{\mathrm{T}}$ and $\tilde{\alpha}_i$ denotes the parameter estimation error with $\tilde{\alpha}_i = \delta\hat{\alpha}_i - \alpha_i$ for i= 1, 2.

In view of Eq.(14), taking the first derivative along the trajectory of the system yields

$$\begin{aligned} \dot{V} &= \boldsymbol{S}^{\mathrm{T}}\boldsymbol{J}^*\dot{\boldsymbol{S}} + \frac{1}{2}\boldsymbol{S}^{\mathrm{T}}\dot{\boldsymbol{J}}^*\boldsymbol{S} + \sum_{i=1}^{2}\frac{1}{\delta\gamma_i}\tilde{\alpha}_i\dot{\tilde{\alpha}}_i + \sum_{i=1}^{2}\frac{K_{\beta_i}^{-1}}{4\delta\gamma_i}\alpha_i^2\beta_i\dot{\beta}_i = \\ &\boldsymbol{S}^{\mathrm{T}}\left\{\frac{1}{2}\boldsymbol{PDEu} + \frac{1}{2}\boldsymbol{P}[\boldsymbol{T}_{\mathrm{d}} + \boldsymbol{D}(\boldsymbol{I}-\boldsymbol{E})\boldsymbol{F}_{\mathrm{f}}] - (\boldsymbol{J}^*\ddot{\boldsymbol{q}}_{\mathrm{r}} + \boldsymbol{C}^*\dot{\boldsymbol{q}}_{\mathrm{r}})\right\} + \\ &\frac{1}{2}\boldsymbol{S}^{\mathrm{T}}(\dot{\boldsymbol{J}}^* - 2\boldsymbol{C}^*)\boldsymbol{S} + \sum_{i=1}^{2}\frac{1}{\delta\gamma_i}\tilde{\alpha}_i\left(-\beta_i^2\hat{\alpha}_i + \gamma_i\|\boldsymbol{Y}_i\|\|\boldsymbol{S}\|\right) + \\ &\sum_{i=1}^{2}\frac{K_{\beta_i}^{-1}}{4\delta\gamma_i}\alpha_i^2\beta_i\dot{\beta}_i \end{aligned} \tag{20}$$

Note that here the fact $\dot{\tilde{\alpha}}_1 = \delta\dot{\hat{\alpha}}_1$ is employed.

From Property 1, we know that $\dot{\boldsymbol{J}}^* - 2\boldsymbol{C}^*$ is a skew-symmetric matrix, and the above equation can be simplified as

$$\begin{aligned} \dot{V} &= \frac{1}{2}\boldsymbol{S}^{\mathrm{T}}\boldsymbol{PDEu} + \frac{1}{2}\boldsymbol{S}^{\mathrm{T}}\boldsymbol{P}[\boldsymbol{T}_{\mathrm{d}} + \boldsymbol{D}(\boldsymbol{I}-\boldsymbol{E})\boldsymbol{F}_{\mathrm{f}}] - \\ &\boldsymbol{S}^{\mathrm{T}}(\boldsymbol{J}^*\ddot{\boldsymbol{q}}_{\mathrm{r}} + \boldsymbol{C}^*\dot{\boldsymbol{q}}_{\mathrm{r}}) - \sum_{i=1}^{2}\frac{1}{\delta\gamma_i}\tilde{\alpha}_i\beta_i^2\hat{\alpha}_i + \\ &\sum_{i=1}^{2}\tilde{\alpha}_i\|\boldsymbol{Y}_i\|\|\boldsymbol{S}\| - \sum_{i=1}^{2}\frac{1}{4\delta\gamma_i}\alpha_i^2\beta_i^2 \end{aligned} \tag{21}$$

After rearranging and collecting the common terms, Eq.(21) can be further simplified as

$$\begin{aligned} \dot{V} &= -\lambda\boldsymbol{S}^{\mathrm{T}}\boldsymbol{J}^*\boldsymbol{S} + \frac{1}{2}\boldsymbol{S}^{\mathrm{T}}\boldsymbol{PDEu} + \\ &\frac{1}{2}\boldsymbol{S}^{\mathrm{T}}\boldsymbol{P}[\boldsymbol{T}_{\mathrm{d}} + \boldsymbol{D}(\boldsymbol{I}-\boldsymbol{E})\boldsymbol{F}_{\mathrm{f}}] - \\ &\boldsymbol{S}^{\mathrm{T}}\left[\boldsymbol{J}^*(\ddot{\boldsymbol{q}}_{\mathrm{r}} - \lambda\boldsymbol{S}) + \boldsymbol{C}^*\dot{\boldsymbol{q}}_{\mathrm{r}}\right] - \sum_{i=1}^{2}\frac{1}{\delta\gamma_i}\tilde{\alpha}_i\beta_i^2(\tilde{\alpha}_i + \alpha_i) + \\ &\sum_{i=1}^{2}\tilde{\alpha}_i\|\boldsymbol{Y}_i\|\|\boldsymbol{S}\| - \sum_{i=1}^{2}\frac{1}{4\delta\gamma_i}\alpha_i^2\beta_i^2 \leq \\ &-\lambda\boldsymbol{S}^{\mathrm{T}}\boldsymbol{J}^*\boldsymbol{S} + \frac{1}{2}\boldsymbol{S}^{\mathrm{T}}\boldsymbol{PDEu} + \frac{1}{2}\|\boldsymbol{S}\|\|\boldsymbol{P}\|\|\boldsymbol{T}_{\mathrm{d}}\| + \\ &\frac{1}{2}\|\boldsymbol{S}\|\|\boldsymbol{P}\|\|\boldsymbol{D}\|\|\boldsymbol{I}-\boldsymbol{E}\|\|\boldsymbol{F}_{\mathrm{f}}\| + \|\boldsymbol{S}\|\|\boldsymbol{J}^*\|\|(\ddot{\boldsymbol{q}} - \lambda\boldsymbol{S})\| + \\ &\|\boldsymbol{S}\|\|\boldsymbol{C}^*\|\|\dot{\boldsymbol{q}}_{\mathrm{r}}\| - \sum_{i=1}^{2}\frac{1}{\delta\gamma_i}\tilde{\alpha}_i^2\beta_i^2 - \sum_{i=1}^{2}\frac{1}{\delta\gamma_i}\tilde{\alpha}_i\beta_i^2\alpha_i + \\ &\sum_{i=1}^{2}\tilde{\alpha}_i\|\boldsymbol{Y}_i\|\|\boldsymbol{S}\| - \sum_{i=1}^{2}\frac{1}{4\delta\gamma_i}\alpha_i^2\beta_i^2 \end{aligned} \tag{22}$$

In view of the Property 2 and Property 3 and the definition in Eq.(15), further simplification of Eq.(22) leads to

$$\begin{aligned} \dot{V} &\leq -\lambda\boldsymbol{S}^{\mathrm{T}}\boldsymbol{J}^*\boldsymbol{S} + \frac{1}{2}\boldsymbol{S}^{\mathrm{T}}\boldsymbol{PDEu} + \|\boldsymbol{S}\|\|\boldsymbol{Y}_1\|\|\boldsymbol{\Theta}_1\| + \\ &\|\boldsymbol{S}\|\|\boldsymbol{Y}_2\|\|\boldsymbol{\Theta}_2\| + \sum_{i=1}^{2}\tilde{\alpha}_i\|\boldsymbol{Y}_i\|\|\boldsymbol{S}\| - \\ &\sum_{i=1}^{2}\frac{1}{\delta\gamma_i}\beta_i^2\left(\tilde{\alpha}_i + \frac{1}{2}\tilde{\alpha}_i\right)^2 \end{aligned} \tag{23}$$

Substituting the control law given by Eq.(16) into the inequality Eq.(23), we can further obtain

$$\begin{aligned} \dot{V} &\leq -\lambda\boldsymbol{S}^{\mathrm{T}}\boldsymbol{J}^*\boldsymbol{S} - \delta\boldsymbol{S}^{\mathrm{T}}\boldsymbol{KS} - \sum_{i=1}^{2}\delta\hat{\alpha}_i\|\boldsymbol{Y}_i\|\|\boldsymbol{S}\| + \\ &\sum_{i=1}^{2}\tilde{\alpha}_i\|\boldsymbol{Y}_i\|\|\boldsymbol{S}\| + \sum_{i=1}^{2}\alpha_i\|\boldsymbol{Y}_i\|\|\boldsymbol{S}\| - \\ &\sum_{i=1}^{2}\frac{1}{\delta\gamma_i}\beta_i^2\left(\tilde{\alpha}_i + \frac{1}{2}\tilde{\alpha}_i\right)^2 \leq \\ &-\lambda\boldsymbol{S}^{\mathrm{T}}\boldsymbol{J}^*\boldsymbol{S} - \delta\boldsymbol{S}^{\mathrm{T}}\boldsymbol{KS} \end{aligned} \tag{24}$$

Therefore, all variables are uniformly bounded. Also because V>0 and $\dot{V} \leq 0$, we can see that $\lim_{t\to\infty} V(t) =$

$V(\infty)$ exists for some finite $V(\infty)\in\mathbf{R}^+$. Also from Eq.(23) and boundedness of all signals within subsequent time derivative of $V(t)$, it is easy to establish that $\ddot{V}(t)\in L_\infty$, or, in other words, uniform continuity for $\dot{V}(t)$. This result, in conjunction with the convergence of $V(t)$ to $V(\infty)$, permits application of Barbalat's lemma (using the alternative statement of this lemma from Ref.[39]) to provide $\dot{V}(t)\to 0$ as $t\to\infty$. This allows us to go further and conclude that $\lim_{t\to\infty}\boldsymbol{S}=\boldsymbol{0}$ and then sliding condition can be guaranteed. From the definition of the sliding surface, the stability of the sliding surface guarantees that the variables $\dot{\boldsymbol{q}}$ and $\boldsymbol{q}$ will also converge to zero. Consequently from the unit-norm constraint on the unit quaternion, we can obtain that $\lim_{t\to\infty} q_0 \neq 0$ (more precisely $\lim_{t\to\infty} q_0 = 1$ is considered here). Then using the identity stated in Eq.(2b), it follows that $\lim_{t\to\infty}\boldsymbol{\omega}=\boldsymbol{0}$. Thus we show that

$$\lim_{t\to\infty}[\boldsymbol{q}\quad \boldsymbol{\omega}\quad \boldsymbol{S}]=\boldsymbol{0} \tag{25}$$

thereby completing the proof of achieving the stated control objective.

Remark 1 From the proceeding analysis, the control law does not need the knowledge of inertia matrix, disturbances and/or their upper bounds for implementation. This fact shows that it is robust to the inertia matrix, which may itself be subject to uncertainties, the external disturbances. The parameters $\hat{\alpha}_i$ (i=1, 2) are estimated on-line using the adaptive algorithm in Eq.(17) starting from any initial value.

Remark 2 From the designed adaptive laws in Eq.(17), a low-pass-filter form of the parameter update law, which makes suitable corrections when the parameters, disturbances and faults are overestimated, ensures that the parameters $\hat{\alpha}_i$ (i=1, 2) are bounded.

Remark 3 From the designed control law in Eqs.(16)-(17), the health condition matrix $\boldsymbol{E}$ and the stuck failure $\boldsymbol{F}_\mathrm{f}$ are not involved in the control scheme, implying that the proposed control law is able to achieve the control objective regardless of the thruster health condition as long as the remaining active thrusters are capable of producing the combined forces sufficient enough to allow the spacecraft to perform a given maneuvering.

Remark 4 From the proceeding proof, although the parameter δ, less than the minimum eigenvalue of matrix $\boldsymbol{DED}^\mathrm{T}$, is involved in stability analysis, an analytical estimate of this parameter is not needed because the proposed control algorithms do not involve such a parameter. But the full-rank requirement for the actuator distribution matrix $\boldsymbol{D}$ should be satisfied such that the stability is ensured only if the matrix $\boldsymbol{DED}^\mathrm{T}$ is positive definite. This requirement can be easily achieved by properly placing the thrusters on the spacecraft[30].

Remark 5 In this control law, an integral feedback is involved, which will achieve zero steady-error in the presence of constant disturbance torques or stuck failures. A detailed discussion of the ability of the integral feedback to reject constant input disturbances specifically for the rigid body attitude control problem can be found in Ref.[40].

Remark 6 In order to avoid the chattering phenomenon due to the imperfect implementation of the sign function in the control law of Eq.(16), the following saturation function

$$\operatorname{sat}\upsilon=\begin{cases}1 & \upsilon>\varepsilon\\ \upsilon & |\upsilon|\le\varepsilon\\ -1 & \upsilon<-\varepsilon\end{cases} \tag{26}$$

is a simple choice to replace the discontinuous function, where ε>0 is a small constant. Note that when the saturation function is introduced, the uniformly ultimately bounded stability will be achieved for the closed-loop system. In the next section, numerical simulation and comparison are given to verify the success of the integral-type sliding mode control (ISMC)-based FTC law in conjunction with the adaptive control technique.

4. Simulation and Comparison Results

To study the effectiveness and performance of the proposed control strategy the detailed response is numerically simulated using the set of governing equations of motion Eqs.(1)-(6) in conjunction with the proposed control laws Eqs.(16)-(17) and Eq.(26). The spacecraft parameter and the external disturbances used in the numerical simulations are shown in Table 1. Note that for all numerical examples considered in this section, the net disturbance torque acting on the system is viewed to be time varying plus constant parts due to gravitation, solar radiation, magnetic force and aerodynamic drags.

In the simulation, four thrusters are assumed to be distributed on the side face of the spacecraft in each corner of the square[41]. The body-fixed y-z plane is orthogonal to the body x axis and at a distance d along the $-x$ axis from the center of mass, and the side length of the thruster assembly is 2c. Thus, the moment arms in the spacecraft body axes are

$$\boldsymbol{r}_1=\begin{bmatrix}-d\\-c\\c\end{bmatrix},\quad \boldsymbol{r}_2=\begin{bmatrix}-d\\c\\c\end{bmatrix},\quad \boldsymbol{r}_3=\begin{bmatrix}-d\\c\\-c\end{bmatrix},\quad \boldsymbol{r}_4=\begin{bmatrix}-d\\-c\\-c\end{bmatrix} \tag{27}$$

To achieve attitude controllability, the thruster directions are canted from the $-x$ axis by ϑ=5° to produce control moment along the x axis. The direction of force generated by each thruster in the body-fixed y-z plane is also different from the principle axes by 45°. As a result, control torques along different axes can be generated and the distribution matrix is indeed:

$$\boldsymbol{D} = \boldsymbol{r}\boldsymbol{n} \tag{28}$$

with $\boldsymbol{r} = [\boldsymbol{r}_1 \quad \boldsymbol{r}_2 \quad \boldsymbol{r}_3 \quad \boldsymbol{r}_4]^{\mathrm{T}}$, $\boldsymbol{n}=[\boldsymbol{n}_1 \quad \boldsymbol{n}_2 \quad \boldsymbol{n}_3 \quad \boldsymbol{n}_4]^{\mathrm{T}}$ and $\boldsymbol{n}_j$ (j =1, 2, 3, 4) being defined as

$$\left.\begin{aligned} \boldsymbol{n}_1 &= [-\cos\vartheta \quad \rho\sin\vartheta \quad \rho\sin\vartheta]^{\mathrm{T}} \\ \boldsymbol{n}_2 &= [-\cos\vartheta \quad -\rho\sin\vartheta \quad \rho\sin\vartheta]^{\mathrm{T}} \\ \boldsymbol{n}_3 &= [-\cos\vartheta \quad -\rho\sin\vartheta \quad -\rho\sin\vartheta]^{\mathrm{T}} \\ \boldsymbol{n}_4 &= [-\cos\vartheta \quad \rho\sin\vartheta \quad -\rho\sin\vartheta]^{\mathrm{T}} \end{aligned}\right\} \tag{29}$$

with $\rho = 1/\sqrt{2}$.

Table 1 Main parameters of a flexible spacecraft

Mission		Imaging the Earth
Inertia moments/(kg·m^2)	Principal moments of inertia	$\boldsymbol{J}_{11}$=1 543.9 $\boldsymbol{J}_{22}$=471.6 $\boldsymbol{J}_{33}$=1 713.3
	Products of inertia	$\boldsymbol{J}_{12}$=−2.3 $\boldsymbol{J}_{13}$=−2.86 $\boldsymbol{J}_{23}$=−35
Orbit	Type	Circular
	Altitude/km	500
	Inclination/(°)	97.4
	Right ascension of ascending node	10:30 a.m.
Attitude control type		Three axis control by four thrusters
Disturbance/(10^{-3}N·m)		T_{d1}=3cos(0.01t)+1 T_{d2}=5sin(0.02t)+3cos(0.025t)+2 T_{d3}=3sin(0.01t)+3
Thruster	Distance d/m	0.5
	Distance c/m	0.2
	The maximum force/N	1.0

Remark 7 Suppose that gas jets (thrusters) produce on-off control actions, while the control signals commanded by the sliding mode controller in Eq.(16) are of continuous type (the discontinuous switching only occurred on the sliding surface). Thus the control signals need to be implemented in conjunction with the on-off actuators. For the discrete type actuators, continuous signals can be converted into equivalent discrete signals by pulse-width pulse-frequency (PWPF) modulation[36]. The key idea of PWPF modulator is to produce a pulse command sequence to the thruster by adjusting the pulse width and pulse frequency. In its linear range, the average torque produced equals the demanded torque input. In this work, we do not go into the details of the characteristics and operation principle of PWPF (interested readers are referred to the Ref.[36] for more details). Therefore, in this work, the PWPF modulation is implemented such that it can be applicable in practice. Furthermore, simulations have been rendered more realistic by considering thruster limit, and it is assumed that the maximum value of control force of thruster (gas jet) is 1.0 N, i.e., $F_{\max}$=0.1 N.

The control gains used in all simulations for adaptive integral sliding model control (AISMC), traditional proportional-integral-derivative (PID) and adaptive sliding model control (ASMC)[30] are shown in Table 2. The performance evaluation of the proposed control strategies presented in this section is divided into four cases: 1) fault-free for attitude maneuvering using three difference control strategies, 2) thruster outage (i.e., one thruster totally fails), 3) thruster stuck failure case I with the 0.5 (−0.5) in value, and 4) thruster stuck failure case II with 1.0 (−1.0) in value. Note that here only the first thruster is considered to be faulty for example. Furthermore, in simulations, the initial attitude quaternion is set at $[q_0 \ \ \boldsymbol{q}^{\mathrm{T}}]^{\mathrm{T}}$=[0.173 648 −0.263 201 0.786 030 −0.526 402]$^{\mathrm{T}}$, and the initial angular velocity is supposed to be $\boldsymbol{\omega}(0)=[0 \quad 0 \quad 0]^{\mathrm{T}}$ (°)/s.

Table 2 Control parameters used for numerical analysis

Control scheme	Controller gain
AISMC	$\boldsymbol{K}$=diag(1 000,1 000,1 000), $\boldsymbol{K}_{\mathrm{P}}=[10]_{3\times3}$, $\boldsymbol{K}_{\mathrm{I}}=[10]_{3\times3}$, $\gamma_1=\gamma_2=10$, $K_{\beta_1}=K_{\beta_2}=50$, ε=0.001
PID controller	$\boldsymbol{K}_{\mathrm{P,PID}}$=diag(1 000,1 000,1 000) $\boldsymbol{K}_{\mathrm{I,PID}}$=diag(0.5,0.5,0.5) $\boldsymbol{K}_{\mathrm{D,PID}}$=diag(3 000,3 000,3 000)
ASMC in Ref.[30]	k_0=30, σ_2=150, β=2, σ_1=0.001, μ=0.2

4.1. Fault-free case

Under the given initial conditions, the designed control laws in Eqs.(16)-(17) and Eq.(26) are first applied to the spacecraft attitude maneuvering with the selected control parameters. Fig.1 (solid line) and Fig.2(a) show the time responses of attitude and thrust demand. As we can see in Figs.1-2, when all thrusters operate under fault-free condition, an acceptable and desirable orientation response is achieved, and the spacecraft reaches the commanded target with a settling time less than 50 s with high accuracy within 10^{-5} in steady-state error as it is shown in Fig.1 (solid

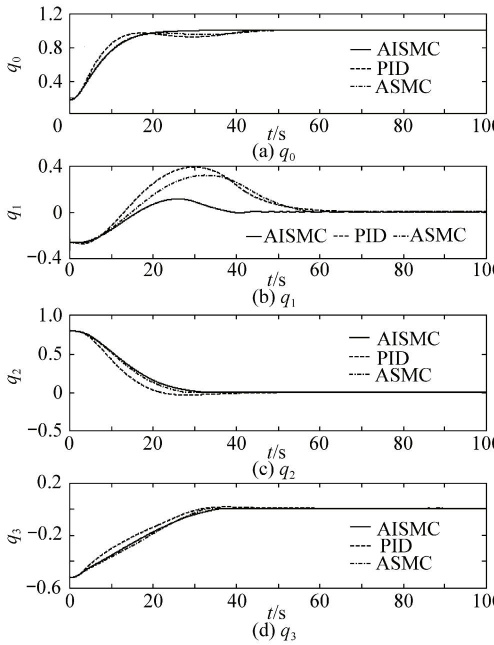

Fig.1 Time response of quaternion under fault-free case.

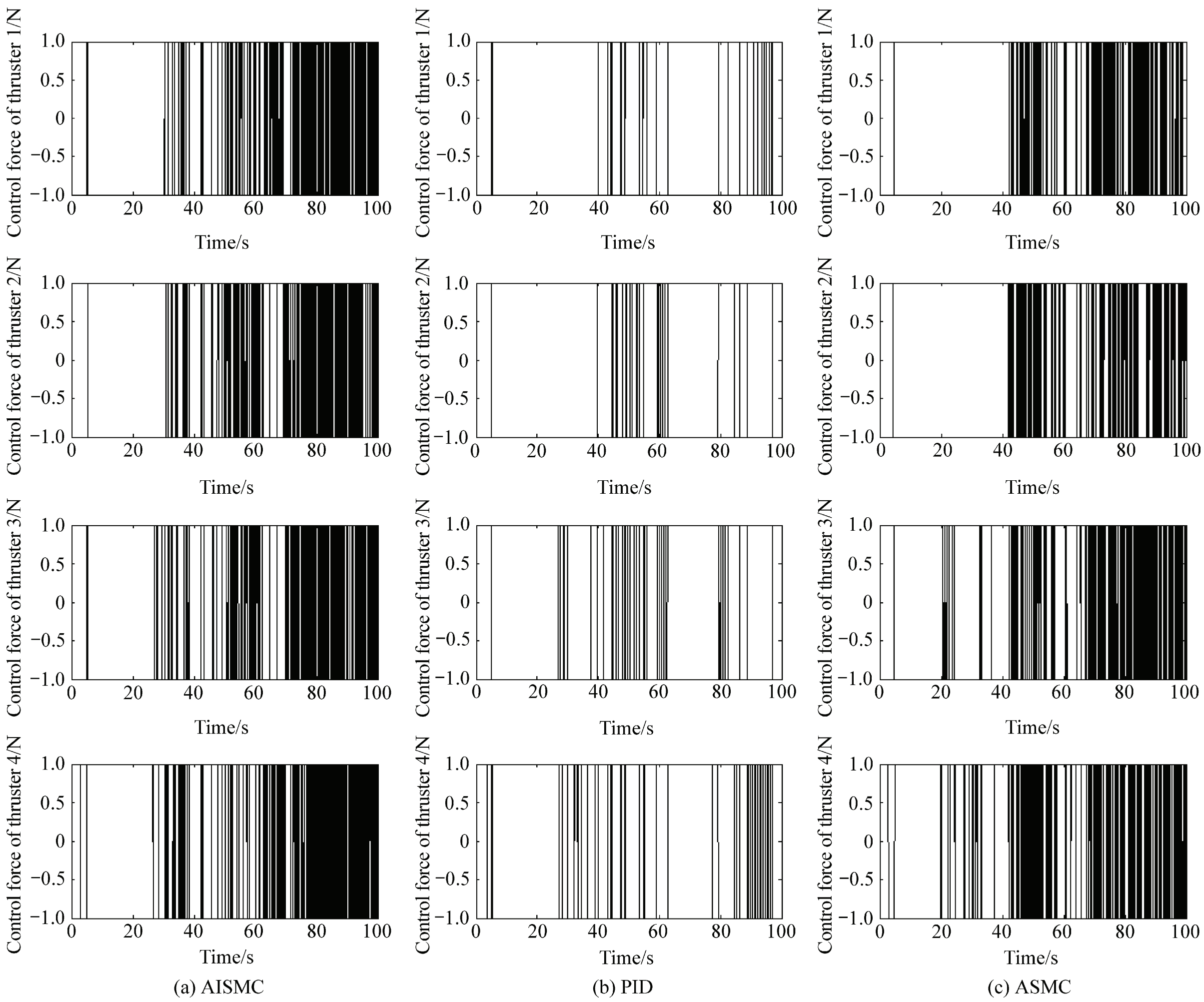

Fig.2 Time response of thruster control forces under fault-free case.

line) .The constant disturbances are also rejected by introducing the integral feedback term in the control law. Note that the restriction on the thruster control force magnitude 1 N is considered explicitly. The adaptive parameter estimates for this case are shown in Fig.3, converging to constant. In addition, simulation is also conducted corresponding to the perturbation of the inertia tensor with $\Delta \boldsymbol{J}= \pm 15\% \boldsymbol{J}$. Smooth responses similar to Fig.1 are observed, so these results are not

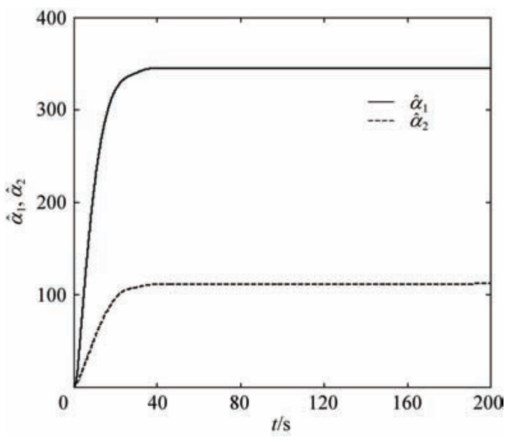

Fig.3 Time response of $\hat{\alpha}_1$ and $\hat{\alpha}_2$ under fault-free case.

shown here. This illustrates that the AISMC is capable of achieving the spacecraft maneuvering target in the presence of disturbances and uncertainties.

For the purpose of comparison, the system is also controlled by using the traditional PID controller. The same simulation cases are repeated with this controller and the results of simulation are shown in Fig.1 (dashed line) and Fig.2(b). For this case, it can be observed that the attitude rotational maneuver can be achieved, but some oscillations exist due to the external disturbances because the robust property is not explicitly considered in the PID control design. Despite the fact that there may exist further room for improvement with better tuning of the control parameter sets, there is not much improvement in the attitude responses.

Comparison with the ASMC in Ref.[30] is further performed for the system. The same simulation case is also repeated and the results of simulation are shown in Fig.1 (dash-dotted line) and Fig.2(c). The control law shows the control ability, to some degree, because of its robustness, as one can see in Fig.1 (dash-dotted line) that the responses of attitude can be improved a lot in comparison with PID case, but with the steady-state error as compared with the proposed method since no integral control term is involved in the feedback loop. From the comparison, the performance of the proposed design is better than the other two controllers even if these designs will adapt to the system parameters under the external disturbances.

4.2. Thruster outage case

In this section, we demonstrate the performance of the proposed control strategies when an abrupt thruster stuck failure, called outage, occurs in the first thruster at the time instant t=5 s. In this case, the control power of the first thruster is completely lost. Figs.4-5 show the results with the same motion commands used in the previous subsections for the proposed, PID and ASMC control methods, respectively. It can be seen that the high control accuracy and good transient process are still obtained for the proposed AISMC; ASMC shows the control ability, to some degree, because of its own robustness to fault even though some steady-state errors exist due to the constant components of disturbances; whereas for PID control, it shows the degradation of performance with much oscillations after the fault occurs. Fig.6 also presents the adaptive parameter estimates for attitude maneuvering to converge to constant when the thruster is subject to abrupt outage fault.

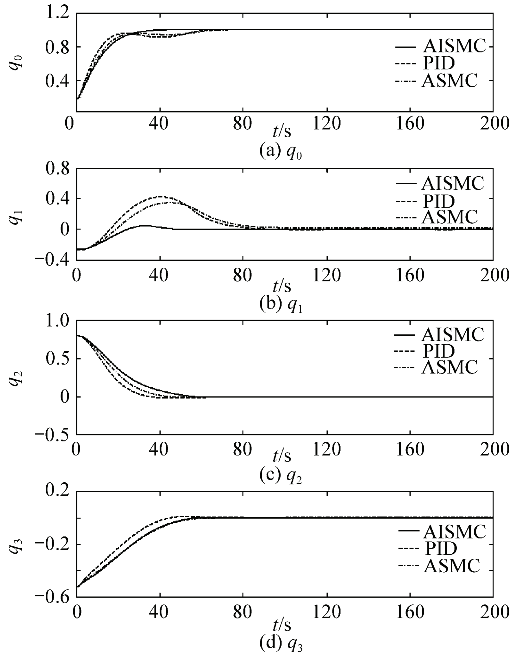

Fig.4 Time response of quaternion under thrust outage case.

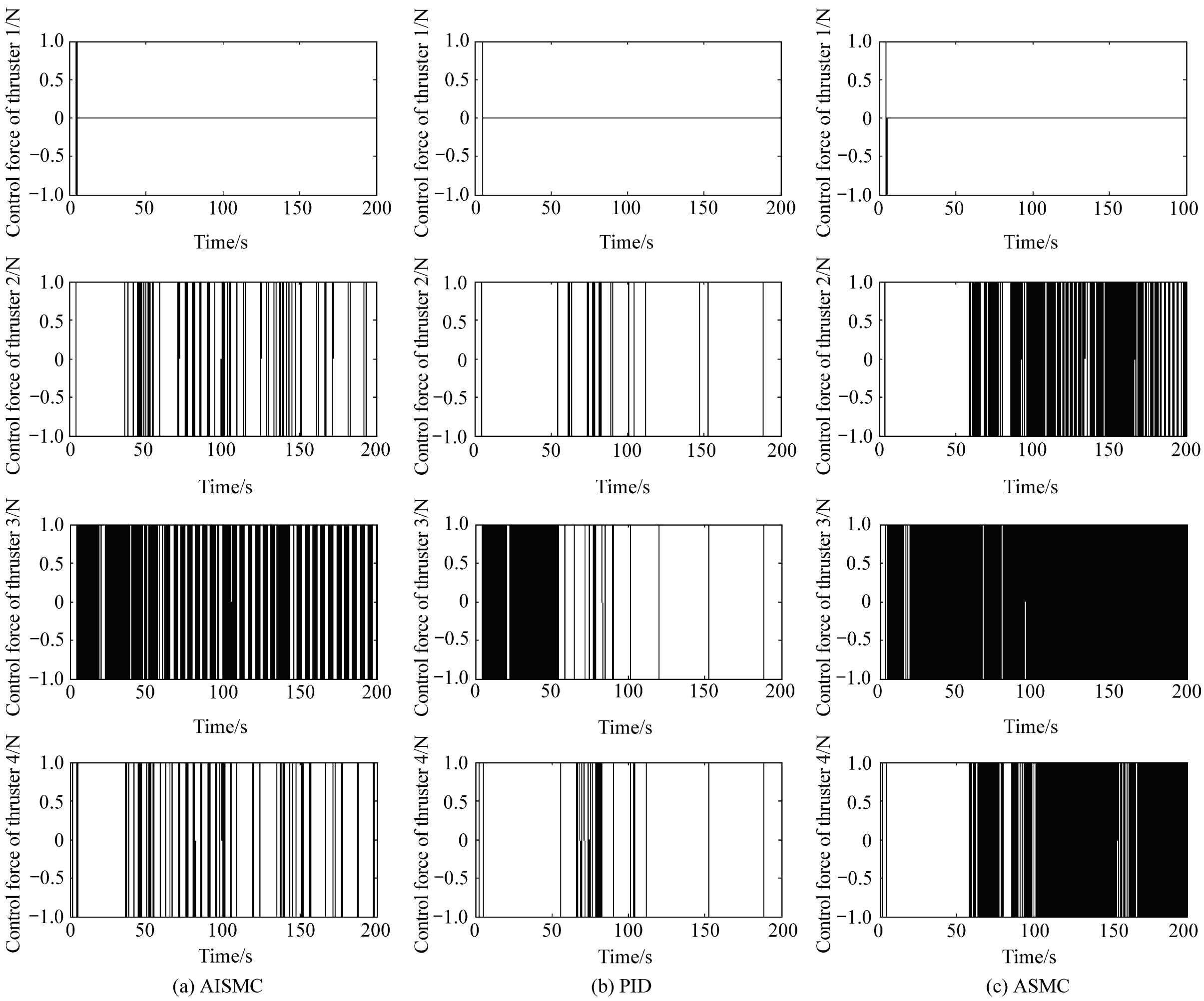

Fig.5 Time response of thruster control forces under thrust outage case.

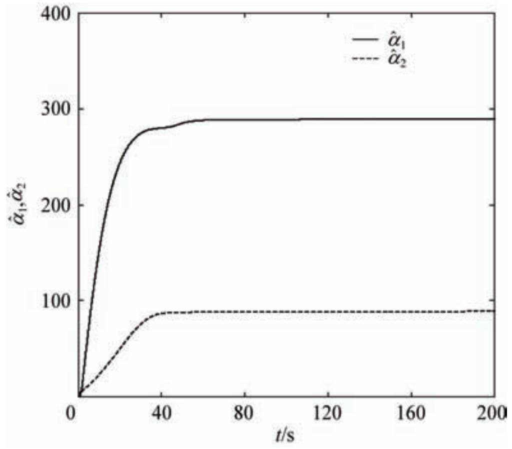

Fig.6 Time response of $\hat{\alpha}_1$ and $\hat{\alpha}_2$ under thrust outage case.

4.3. Stuck failure case I

In this subsection, we assess the case in which the first thruster is stuck at a certain position, for example at 0.5 in value. The effect of such fault can be viewed as additional constant disturbances imposed on the system. Under the same initial conditions and control parameters, the simulation is repeated with this kind of fault. Figs.7-8 present the attitude and control forces responses using the three different control schemes. It

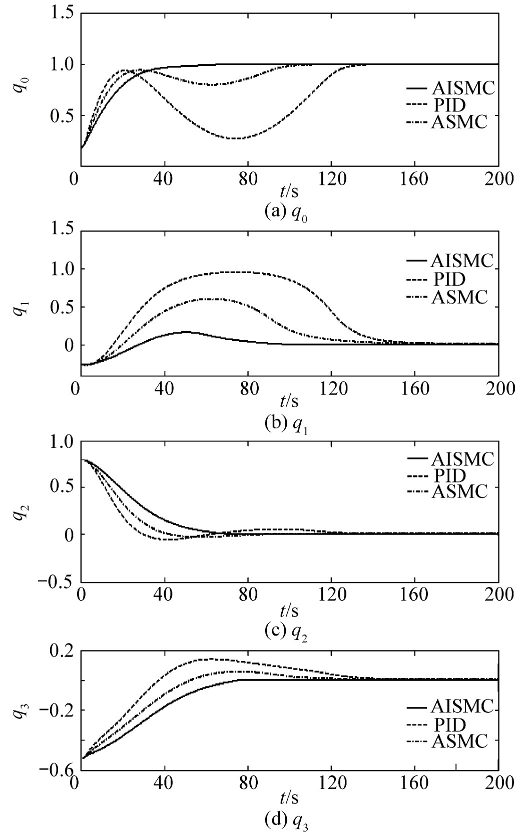

Fig.7 Time response of quaternion under stuck failure case I.

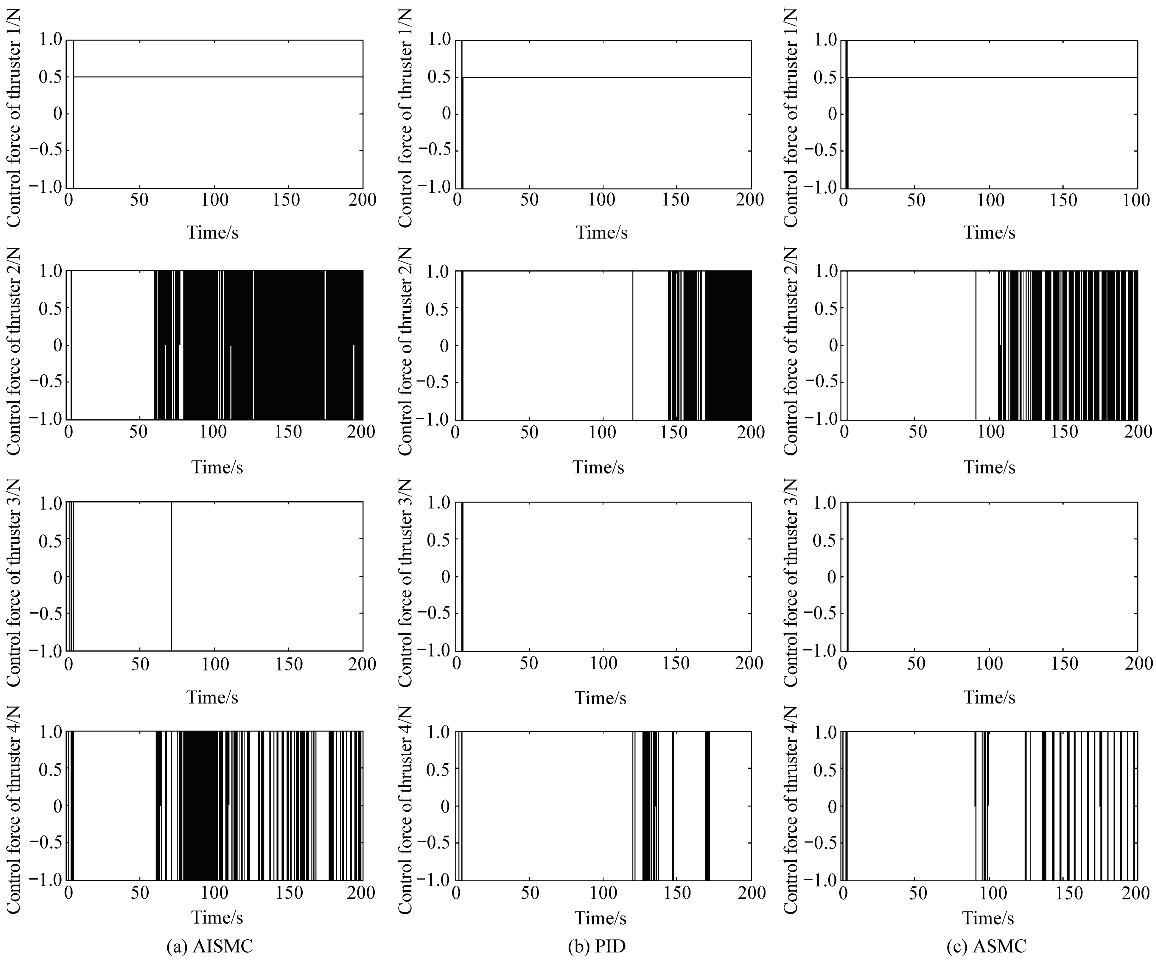

Fig.8 Time response of thruster control forces under stuck failure case I.

is seen that fairly good control performance is achieved under this severe scenario even though more settling time (about 100 s) is required due to the constant-like disturbance for the proposed controller; for the ASMC, severe oscillations can be observed and also with large steady-state error in the range of 0.01 in value; while for PID case, it exhibits poor performance in maneuvering even if the integral control term is introduced in the feedback loop, and no fault tolerance design is considered explicitly in the system design. Fig.9 also presents the adaptive parameter estimates when the abrupt stuck occurs at t=5 s. In addition, to examine the sensitivity of the controller to the stuck at a certain position in inverse direction, simulation is done corresponding to the stuck at −0.5 in value. Similar responses compared with Figs.7-9 are obtained, so they are omitted here for space limitation.

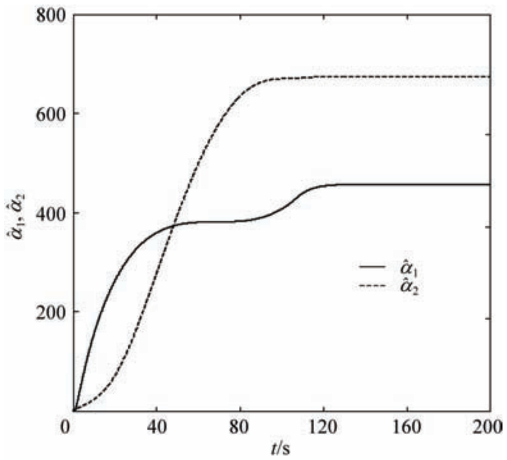

Fig.9 Time response of $\hat{\alpha}_1$ and $\hat{\alpha}_2$ under stuck failure case I.

4.4. *Stuck failure case II*

In this case, an even more severe fault scenario than the previous case is considered with the stuck at 1.0 in value. Figs.10-11 show the simulation resuts under the same initial conditions and controller parameters. We can see the degradation of maneuvering performance after occurrence of this severe fault, but the system can be stabilized after 160 s; while for the ASMC or PID case, the system becomes unstable, in which this kind of fault cannot be tolerant even if the design of ASMC explicitly takes the fault into account. The adaptive parameters increase instantaneously to cope with the poor performance and the convergence speed of the AISMC can be observed in Fig.12 under this fault. Note that varying the control gains for AISMC can improve its performance, but to compare these control laws, it is important to keep the gains unchanged (as shown in Table 2) for all simulation cases. In addition, to examine the sensitivity of the controller to the stuck at a certain position in inverse direction, simulation is conducted corresponding to the stuck at −1.0 in value. Similar responses compared with Figs.7-9 are obtained, so they are omitted here.

As can be seen from the simulation results in the above two cases under stuck failures, stuck failures are even more difficulty to be handled compared with the outage failure case since their adverse effects add constant disturbances to the system. For more severe failures, better performances of the proposed AISMC scheme over ASMC and PID have been achieved.

Summarizing all the cases (normal case and fault cases), it is noted that the proposed controller design method can improve the normal performance more significantly than the PID or ASMC method in both theory and simulations. Also, in fault cases simulated in this article, the proposed method has better results than those of existing controllers. It can also be observed that as more severe fault cases are considered in the design, the proposed controller can still guarantee system to be stable. In addition, extensive simulations are also conducted using different control parameters, disturbance inputs and parameter uncertainties. These results show that in the closed-loop system, attitude control is accomplished in spite of these undesired effects in the system. Moreover, the flexibility in the choice of control parameters can be utilized to obtain desirable performance while meeting the constraints on the control magnitude. These control schemes provide a theoretical basis for the practical application of the advanced control theory to future spacecraft attitude control system design.

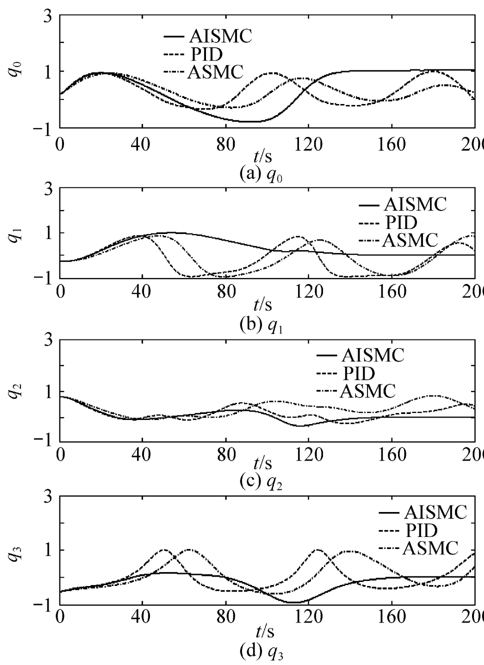

Fig.10 Time response of quaternion under stuck failure case II.

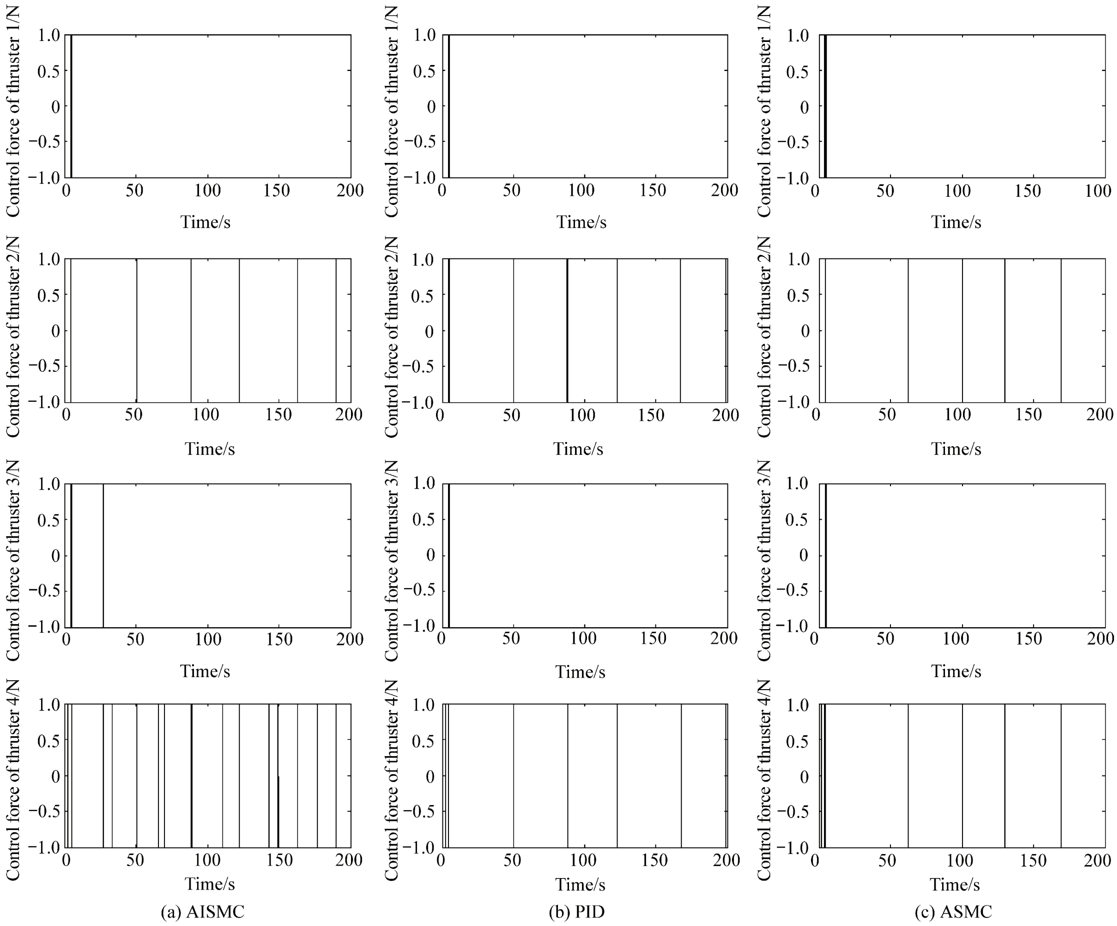

Fig.11 Time response of thruster control forces under stuck failure case II.

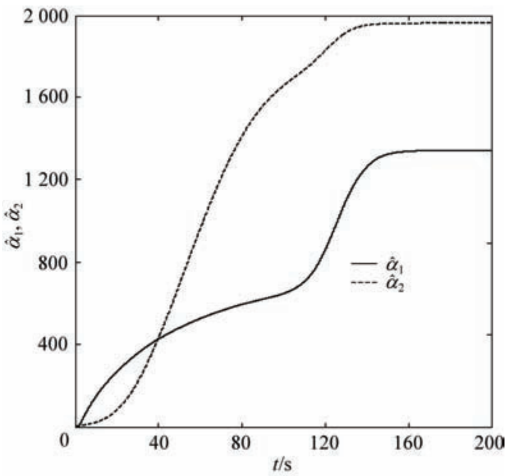

Fig.12 Time response of $\hat{\alpha}_1$ and $\hat{\alpha}_2$ under stuck failure case II.

5. Conclusions

An adaptive integral sliding mode-based FTC scheme has been developed for spacecraft attitude maneuvering using redundant (four) thrusters in the presence of parametric uncertainties, disturbances and even unknown stuck failures. The proposed control design method does not require the system identification process to identify the faults as well as the process of fault detection and isolation. The control formulation is based upon Lyapunov's direct stability theorem, the globally asymptotically stability of closed-loop system is ensured, and the robustness to disturbances and unknown stuck failures is also guaranteed provided that appropriate robustness conditions imposed on the controller gains are satisfied. Moreover, by including the integral feedback term, the designed controller can reject the constant components of disturbances and also tolerate actuator stuck failures. The control designs are evaluated using numerical simulation comparisons between the developed approach and other referred schemes, where the expected performances have been shown. In the simulations, several different types of reaction thruster failure scenarios are investigated. Based upon the results presented in this article, it is concluded that the proposed control scheme successfully handles failures if one thruster wheel fails completely, or is stuck at certain unknown positions. While the simulation results presented in this article merely illustrate formulations for a particular attitude maneuver, further testing would be required to reach any conclusions about the efficacy of the control and adaptation laws for tracking arbitrary maneuvers. In addition, this FTC scheme places no restriction explicitly on the magnitude of the desired control, and the design with explicitly considering the actuator saturation limit is also under investigation. Future work is planned to study the digital implementation of such control scheme on hardware platforms for attitude control experimentation.

References

[1] Singh S N. Rotational maneuvers of nonlinear uncertain spacecraft. IEEE Transactions on Aerospace Electronic and Systems 1988; 24(2): 114-123.

[2] Nagata T, Modi V J, Matsuo H. Dynamics and control of flexible multi-body systems Part II: simulation code and parametric studies with nonlinear control. Acta Astronautica 2001; 49(11): 595-610.

[3] Karray F, Grewal A, Glaum M, et al. Stiffening control of a class of nonlinear affine systems. IEEE Transactions on Aerospace Electronic and Systems 1997; 33(2): 473-484.

[4] Tsiotras P. Further passivity results for the attitude control problem. IEEE Transactions on Automatic Control 1998; 43(11): 1597-1600.

[5] Hokayem P F, Schilling K. Input-to-state stable attitude control. Journal of Guidance, Control, and Dynamics 2008; 31(6): 1826-1829.

[6] Hu Q L, Ma G F. Variable structure control and active vibration suppression of flexible spacecraft during attitude maneuver. Aerospace Science and Technology 2005; 9(4): 307-317.

[7] Iyer A, Singh S N. Variable structure slewing control and vibration damping of flexible spacecraft. Acta Astronautica 1991; 25(1): 1-9.

[8] Hu Q L. Sliding mode maneuvering control and active vibration damping of three-axis stabilized flexible spacecraft with actuator dynamics. Nonlinear Dynamics 2008; 52(3): 227-248.

[9] Singh S N, Araujo A D. Adaptive control and stabilization of elastic spacecraft. IEEE Transactions on Aerospace and Electronic Systems 1999; 35(1): 115-122.

[10] Maganti G B, Singh S N. Simplified adaptive control of an orbiting flexible spacecraft. Acta Astronautica 2007; 61(7-8): 575-589.

[11] Singh S N, Zhang R. Adaptive output feedback control of spacecraft with flexible appendages by modeling error compensation. Acta Astronautica 2004; 54(4): 229-243.

[12] Hu Q L, Shi P, Gao H J. Adaptive variable structure and commanding shaped vibration control of flexible spacecraft. Journal of Guidance, Control, and Dynamics 2007; 30(3): 804-815.

[13] Zeng Y, Araujo A D, Singh S N. Output feedback variable structure adaptive control of a flexible spacecraft. Acta Astronautica 1999; 44(1): 11-22.

[14] Hu Q L, Ma G F. Adaptive variable structure maneuvering control and vibration reduction of three-axis stabilized flexible spacecraft. European Journal of Control 2006; 12(6): 654-668.

[15] Subbarao K. Nonlinear PID-like controllers for rigid-body attitude stabilization. The Journal of the Astronautical Sciences 2004; 52(1-2): 61-74.

[16] Hu Q L, Cao J, Zhang Y Z. Robust backstepping sliding mode attitude tracking and vibration damping of flexible spacecraft with actuator dynamics. ASCE Journal of Aerospace Engineering 2009; 22(2): 122-135.

[17] Zhang Y M, Jiang J. Bibliographical review on reconfigurable fault-tolerant control systems. Annual Reviews in Control 2008; 32(2): 229-252.

[18] Benosman M. A survey of some recent results on nonlinear fault tolerant control. Mathematical Problems in Engineering 2010; 2010: 1-25. DOI: 10.1155/2010/586169.

[19] Hsieh C S. Performance gain margins of the two-stage LQ reliable control. Automatica 2002; 38(11): 1985-1990.

[20] Ye D, Yang G H. Adaptive fault-tolerant tracking control against actuator faults with application to flight control. IEEE Transactions on Control Systems Technology 2006; 14(6): 1088-1096.

[21] Tang X D, Tao G, Joshi S M. Adaptive actuator failure compensation for nonlinear MIMO systems with an aircraft control application. Automatica 2007; 43(11): 1869-1883.

[22] Zhang Y M, Jiang J. An active fault-tolerant control system against partial actuator failures. IEE Proceedings Control Theory and Applications 2002; 149(1): 95-104.

[23] Alwi H, Edwards C. Fault detection and fault-tolerant control of a civil aircraft using a sliding-mode-based scheme. IEEE Transactions on Control Systems Technology 2008; 16(3): 499-510.

[24] Kim D, Kim Y. Robust variable structure controller design for fault tolerant flight control. Journal of Guidance, Control, and Dynamics 2000; 23(3): 430-437.

[25] Bošković J D, Li S M, Mehra R K. Intelligent control of spacecraft in the presence of actuator failures. Proceedings of the 38th IEEE Conference on Decision and Control. 1999; 4472-4477.

[26] Li L, Ma L Y, Khorasani K. A dynamic recurrent neural network fault diagnosis and isolation architecture for satellite's actuator/thruster failures. Lecture Notes in Computer Science 2005; 3498(3): 574-583.

[27] Wu Q, Saif M. Robust fault diagnosis for a satellite large angle attitude system using an iterative neuron PID observer. Proceedings of the American Control Conference. 2006; 5710-5715.

[28] Chen W, Saif M. Observer-based fault diagnosis of satellite systems subject to time-varying thruster faults. Journal of Dynamic Systems, Measurement, and Control 2007; 129(3): 352-356.

[29] Jin J H, Ko S H, Ryoo C K. Fault tolerant control for satellites with four reaction wheels. Control Engineering Practice 2008; 16(10): 1250-1258.

[30] Cai W C, Xiao X L, Song Y D. Indirect robust adaptive fault-tolerant control for attitude tracking of spacecraft. Journal of Guidance, Control, and Dynamics 2008; 31(5): 1456-1463.

[31] Hu Q L. Robust adaptive sliding-mode fault-tolerant control with L_2-gain performance for flexible spacecraft using redundant reaction wheels. IET Control Theory & Applications 2010; 4(6): 1055-1070.

[32] Chen W, Jiang J. Fault-tolerant control against stuck actuator faults. IEE Proceedings Control Theory & Applications 2005; 152(2): 138-146.

[33] Yang G H, Wang H, Xie L H. Fault detection for output feedback control systems with actuator stuck faults: a steady-state-based approach. International Journal of

Robust Nonlinear Control 2010; 20(15): 1739-1757. DOI: 10.1002/rnc.1546.

[34] Zhao Q, Jiang J. Reliable state feedback control system design against actuator failures. Automatica 1998; 34(10): 1267-1272.

[35] Yang G H, Kim K Y. Fault-tolerant flight tracking control with stuck faults. Proceedings of American Control Conference. 2003; 521-526.

[36] Sidi M J. Spacecraft dynamics and control. Cambridge: Cambridge University Press, 1997.

[37] Costic B T, Dawson D M, de Queiroz M S, et al. Quaternion based adaptive attitude tracking controller without velocity measurements. Journal of Guidance, Control, and Dynamics 2001; 24(6): 1214-1222.

[38] Stepanenko Y, Cao Y, Su C Y. Variable structure control of robotic manipulator with PID sliding surfaces. International Journal of Robust and Nonlinear Control 1998; 8(1): 79-90.

[39] Ioannou P A, Sun J. Stable and robust adaptive control. Upper Saddle River: Prentice-Hall, 1995.

[40] Schaub H, Junkins J L. Analytical mechanics of space systems (AIAA education series). Reston: AIAA, 2003.

[41] Show L L, Juang J C, Jan Y W. An LMI-based nonlinear attitude control approach. IEEE Transactions on Control Systems Technology 2003; 11(1): 73-83.

Biography:

HU Qinglei Born in 1979, he received his B.E. degree in 2001 from the Department of Electrical and Electronic Engineering at Zhengzhou University, P.R. China, and M.E. and Ph.D. degrees from the Department of Control Science and Engineering at Harbin Institute of Technology with specialization in controls, P.R. China, in 2003 and 2006, respectively. Since 2003, he has been working in the Department of Control Science and Engineering at Harbin Institute of Technology and was promoted to associate professor in 2006. He worked as a postdoctoral research fellow at the School of Electrical and Electronic Engineering, Nanyang Technological University of Singapore from 2006 to 2007. From 2008 to 2009, he visited University of Bristol of UK as Senior Research Fellow supported by Royal Society Fellowship. He is currently working as a research associate in the Department of Mechanical and Industrial Engineering, Concordia University of Canada. His research interests include variable structure control & applications, robust control & applications, spacecraft fault tolerant control & applications. In these areas, he has published more than 40 technical papers. He was an associate editor for the Journal of the Franklin Institute.

E-mail: huqinglei@hit.edu.cn